

The impact of benthic microbial communities in sediment dispersion and bedform preservation: a view from the oldest microbially induced sedimentary structures in South America

Lucas Veríssimo Warren^{1*} , Filipe Giovanini Varejão² , Fernanda Quaglio³ , Lucas Inglez¹ ,
Fernanda Buchi¹ , Marcello Guimarães Simões⁴ 

Abstract

The influence of microbial communities upon sedimentary dynamics is an issue of increasing significance. Over the last decades, studies have revealed a particular class of sedimentary structures and textures produced by the interaction among distinct flows, marine substrate, and benthic microbial communities. We present evidence of the oldest record of microbially-induced sedimentary structures (MISS) in South America, as recorded in low-grade metasedimentary rocks of the Early Mesoproterozoic ($\sim 1536 \pm 33$ Ma) Tiradentes Formation, state of Minas Gerais, SW Brazil. Types 1, 2, and 3 correspond to wrinkle, pustular, and dome structures related to flat or rippled bed surfaces, preserved in metasediments deposited in shallow marine settings. Evidence supporting the microbial origin of these structures includes delicate morphology, degree of alignment, presence of original mat cover, and orientation of quartz grains indicating biostabilization. The presence of distinct MISS associated with well-preserved ripple marks, wrinkled surfaces, and flatbeds suggests deposition under varied energy conditions with different potentials for the preservation of surficial structures. Vertical growth of microbial communities influences sediment cohesion and stability. This reduces substrate roughness and, as a consequence, wave and current shear, thereby increasing the preservation potential of bedforms and delicate features of their bedding surfaces.

KEYWORDS: Mesoproterozoic; microbially-induced sedimentary structures; MISS morphogenesis; siliciclastic rocks; marine transitional settings.

INTRODUCTION

The role of biofilms in the preservation of ripple marks

Microbial communities were widespread in the Precambrian before the rise of metazoans and their predatory grazing habit (Gehling 1999, Seilacher 1999, Riding 2006), reaching its climax in morphotype richness as of the end of the Paleoproterozoic

and Mesoproterozoic Eras (Awramik and Sprinkle 1999). These microbial colonies thrived in the ocean substrate by organizing themselves in benthic, complex, and stratified arrangements, developing deposits generally called microbialites (Burne and Moore 1987). A thin and organized coat of microbial communities and extracellular polymeric substances (EPS) form the biofilms that colonized and covered the substrate of marine and transitional sedimentary environments (Davey and O'Toole 2000, Decho 2000). Notably, these biofilms were recognized to interact with the surface sediments, modifying them and inducing a variety of textures (Davies *et al.* 2016), known as microbially-induced sedimentary structures (MISS, *sensu* Noffke *et al.* 1996). Furthermore, benthic microbial communities can interact with physical sedimentary dynamics in both marine and non-marine environments, promoting substrate stabilization and preserving a series of sedimentary structures (Noffke and Awramik 2013).

The preservation of ripple marks is controlled by the rapid deposition of sediments, followed by mud/silt deposition or biofilm cover (Deckere *et al.* 2001, Noffke *et al.* 2001, Friend *et al.* 2008, Noffke 2010, Davies *et al.* 2016, Tarhan 2018, Baas *et al.* 2019, Cuadrado 2020). Also, the wavelength of ripples is provenly controlled by the presence of cohesive EPS (Baas *et al.* 2019). The role of biofilms in the preservation of such structures has been investigated since the early works of Neumann *et al.* (1970), who demonstrated their biostabilization characteristics.

Supplementary data

Supplementary data associated with this article can be found in the online version: [Supplementary Material](#).

¹Departamento de Geologia, Instituto de Geociências e Ciências Exatas, Universidade Estadual Paulista “Júlio de Mesquita Filho” – Rio Claro (SP), Brazil. E-mails: lucas.warren@unesp.br, lucas.inglez@hotmail.com, fernandabuchi@gmail.com, profmgsimoes@gmail.com

²Departamento de Geologia, Escola de Minas, Universidade Federal de Ouro Preto – Ouro Preto, (MG), Brazil. E-mail: filipe.varejao@hotmail.com

³Departamento de Ecologia e Biologia Evolutiva, Universidade Federal de São Paulo – Diadema (SP), Brasil. E-mail: quaglio@gmail.com

⁴Instituto de Biociências, Departamento de Zoologia, Universidade Estadual Paulista “Júlio de Mesquita Filho” – Rio Claro (SP), Brazil.

*Corresponding author.



More recently, the interaction between physical (i.e., hydraulic energy) and biological (i.e., presence of biofilms) parameters have been shown to control the preservation and mobility of distinct types of ripples (Friend *et al.* 2008, Baas *et al.* 2019, Cuadrado 2020, Scheidweiler *et al.* 2021). However, the exact mechanisms of interaction between variations in the hydraulic gradient, sedimentary particle grain size, and generation/preservation of the associated bedforms are still not fully understood. Likewise, the quantification and discussion of the noteworthy abundance and preservation of bedforms (including ripple marks) throughout the Precambrian sedimentary record (examples in Tarhan 2018, Basilici *et al.* 2020, Bayet-Goll and Daraei, 2020, Sarkar *et al.* 2020) are geological issues of growing interest worldwide.

A case study: metasandstone of the Tiradentes Formation, SW Brazil

The Brazilian town of Tiradentes, state of Minas Gerais, Brazil, listed as a National Heritage site, is a historical centennial town with streets covered by decimeter to meter metasandstone slabs that are surprisingly well-preserved and have abundant and diverse ripple marks on their surface. These stones were originally mined by 18th-century workers in a nearby quarry where a Mesoproterozoic succession of shallow marine conditions with a great and diverse amount of ripple cross-laminated metasandstone is fully exposed. These belong to the Tiradentes Formation, São João del Rei Basin, São Francisco Craton (Ribeiro 1997). Upon the ripple mark-rich bedding planes, the occurrence of associated sedimentary surface textures (SST *sensu* Davies *et al.* 2016) of distinct types is striking. Herein, we present a stratigraphic, sedimentologic, and detailed morphologic analysis of these well-preserved examples of SST, aiming to explore the relationship between surface textures and bedforms. Thus, the main questions this investigation sought to answer included: did the presence of SST influence the origin and preservation of ripple marks? Is there any variation in the quality/type of preservation regarding changes in the hydraulic regime, granulation, and categories of associated SST? Is there a correlation between the presence of SST and increased ripple preservation during the Mesoproterozoic?

GEOLOGICAL SETTING

The Early Mesoproterozoic (1536 ± 33 Ma and 1540 ± 45 Ma) Tiradentes Formation from the São João del Rei Basin is located southeast of the São Francisco Craton (Fig. 1A), and chronologically correlated with the second extensional cycle of the Espinhaço Supergroup (Ribeiro *et al.* 2013). From a geotectonic perspective, the Espinhaço Supergroup comprises the basal deposits of an intracontinental rift system developed within the southern part of the São Francisco-Congo Craton (Teixeira *et al.* 2000). A connection between the São João del Rei and Espinhaço basins is suggested based on age and tectonostratigraphic relationships, characterizing the successions as part of regional-scale polycyclic and asymmetric aulacogens (Martins-Neto 2000, Ribeiro *et al.* 2013).

The ~1,000 m-thick, shallow marine Tiradentes Formation (Fig. 1B) is composed, from the base to the top, by the Tiradentes, São José, Tejuco, and Lenheiro sequences (Ribeiro *et al.* 2013). The Tiradentes Formation is exclusively constituted by terrigenous low-grade metamorphic rocks (low greenschist) resting unconformably above the Paleoproterozoic basement of the Mineiro Belt (Ribeiro *et al.* 1990). In the southern part of the state of Minas Gerais, the NE-SW São José Ridge reaches a length of 13.5 km and is an impressive mountain range, rising approximately 1,100 m above sea level (Ribeiro 1997, Soares *et al.* 2002). There, the whole succession crops out as non-weathered and weakly metamorphized rocks (Fig. 1C).

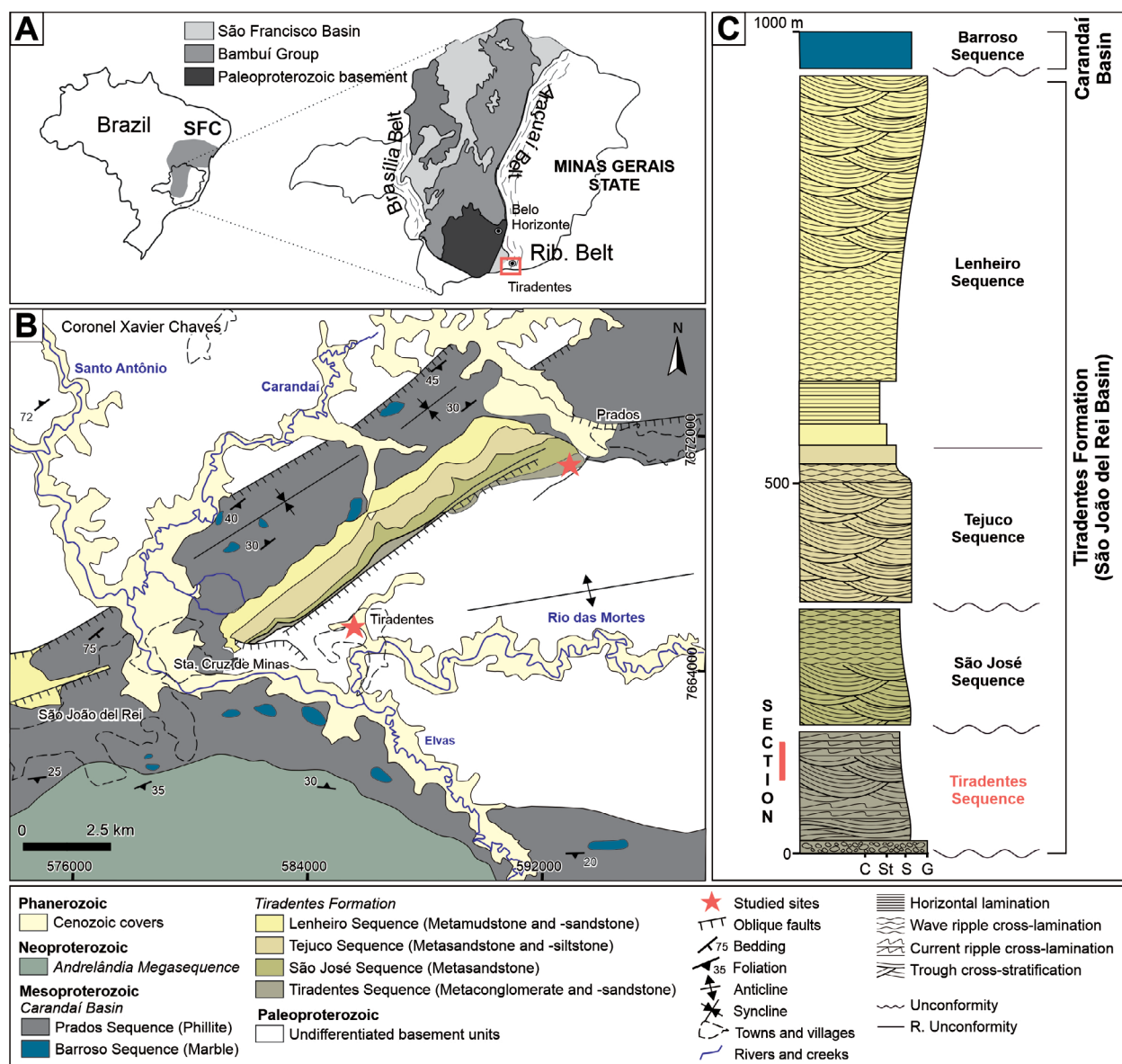
In the study area, comprising the eastern segment of the São José Ridge and between the towns of Tiradentes and Prados (Fig. 1B), the lower ~150 m-thick Tiradentes Sequence (Ribeiro 1997, Ribeiro *et al.* 2013) comprises massive metaconglomerate and cross-bedded pebbly metasandstone with isolated occurrences of thin-bedded iron formations at the base, and trough cross-bedded and ripple cross-laminated metasandstone at the top (Ribeiro *et al.* 2013). The Tiradentes Sequence is interpreted as deposited in a shoreface to foreshore shallow marine environment, characterizing a regional transgression over a denuded basement (Ribeiro *et al.* 2013). The paleocurrents indicate a NE-SW coastline with an open oceanic connection probably toward SE (Ribeiro *et al.* 2003). The intermediate shoreface/foreshore São José and Tejuco sequences are characterized by fine to medium-grained metasandstone presenting trough cross-stratification, horizontal stratification, ripple cross-lamination, and rare swalley/hummocky cross-stratification (Ribeiro 1997, Soares *et al.* 2002). At the top, the ~450 m-thick deltaic succession of the Lenheiro Sequence (Ribeiro 1997) is composed of metamudstone, metasandstone, and metaconglomerate, which are bounded at the top by an angular non-conformity with the upper Barroso Sequence (Ribeiro 1997, Ribeiro *et al.* 2013) (Fig. 1C). The Barroso Sequence is interpreted to be deposited under quiescent tectonic settings, probably representing the installation of a passive margin (sag) basin (Ribeiro *et al.* 2013).

MATERIAL AND METHODS

The best initial approach to study the sedimentary surface textures (SST, *sensu* Davies *et al.* 2016) in metasandstone of the Tiradentes Formation is the direct observation of these particular structures in the paving stones of the historic streets of Tiradentes town, state of Minas Gerais, where a pleasant walk reveals distinct preservation SST in ripple marks of different scales (see Figs. 2A and 2B). After careful historical research in the Historical and Geographical Institute of Tiradentes, we found that the streets were originally paved in the mid 18th century by enslaved laborers. After that, the streets were partially repaved in 1959, keeping their original aspect until today. During street paving renovation, thousands of rock slabs were collected from an old quarry located in the eastern part of the São João Ridge, near the town of Prados (Figs. 1 and 2C and 2D). Many of these paving slabs correspond to metasandstone from the Tiradentes Sequence, the basal succession of the Tiradentes Formation, some of them presenting wave and current ripples with very well-preserved SST on their surface.

The analysis of available satellite images, historical aerial photos, and geologic maps revealed that the original site of the abandoned quarry is presently situated in the São José Ridge Environmental Protection Area. In this quarry, a detailed columnar section (1:50) was measured, and the lithologies, bed geometries, and structures were described. After that, the data were systematized in distinct sedimentary facies (according to the protocol of Miall 2006). The presence of non-weathered exposure also allowed relatively fresh SST-bearing rocks to be sampled for further petrographic analysis. Yet, a large number of paleocurrent data from the intermediate succession of the Tiradentes Sequence were also obtained. All paleocurrent data are represented in *Clar* notation and the correct position of individual slabs (depositional surface in normal position) was determined by using way-up (geopetal) structures such as graded bedding, sole marks, ripple marks, and cross-bedding.

Much of the description and classification of SST were performed in the paving slabs from the historic streets of Tiradentes, where these structures are exceptionally well preserved (i.e. presenting diagnostic macroscopic morphological features). To avoid weathered samples, we only selected metasandstone slabs with no evidence of granular disintegration, flaking, and micro-delamination (Smith *et al.* 2005). Paving rock slabs showing signs of natural or anthropic erosion were also avoided and only very-well preserved samples were considered for the analysis. All the individual slabs analyzed (n = 306) were cataloged and described regarding lithology, presence (or absence) of wave or current ripples, presence (or absence) of SST, and the type of SST. The description and classification of SST were based on several examples found in the specific literature, and compared to primary, microbially-induced sedimentary structures (MISS, McIlroy and Walter 1997, Noffke 2009, 2010, 2018, Noffke *et al.* 1996, Noffke



Source: modified from Ribeiro *et al.* (2003, 2013).

SFC: São Francisco Craton; Rib. Belt.: Ribeira Belt; C: clay; St: silt; S: sand; G: gravel.

Figure 1. Location and stratigraphic position of the studied succession. (A) São Francisco Craton and the study area location in the state of Minas Gerais, Brazil. (B) Geological map of the São José Ridge, showing the location, in the eastern section of the studied sites (red stars). (C) Schematic columnar section of the São João del Rei Basin and the base of the Carandaí Basin. The detailed columnar section of Fig. 3 was acquired in the intermediate/upper part of the basal Tiradentes Sequence.

et al. 2001, Hagadorn and Bottjer 1999, Porada and Bouougrí 2007, Porada *et al.* 2008, Kumar and Ahmad 2014, Menon *et al.* 2015, Menon *et al.* 2016, Davies *et al.* 2016).

The microscopic classification of rocks followed Folk (1980) the sedimentary lithotypes. Due to the presence of incipient low-grade metamorphism in the rocks described, their denomination was preceded by the prefix “meta”. The petrographic analysis allowed the macroscopic description to be refined and several microstructures to be identified in the rock framework, possibly related to substrate stabilization promoted by either epi- or endobenthic microbial communities. All laboratory procedures were performed in the facilities of the Department of Geology, Universidade Estadual Paulista “Júlio de Mesquita Filho” (UNESP), Rio Claro, Brazil.

SEDIMENTARY SUCCESSION

The paving stones on the streets of Tiradentes taken from an abandoned quarry near the town of Prado in the eastern part of the São José Ridge (Fig. 1) were extracted from the uppermost part of the Tiradentes Sequence, which crops out with an exposure of ca. 20 m (Fig. 3), where five sandstone-dominated sedimentary facies were described (Tab. 1).

At the base, the sedimentary pile studied is characterized by a 5.8 m-thick, fining-upward succession of four facies of

metasandstone with different structures (see Tab. 1). Meter-thick tabular beds of planar cross-stratified (S_p), dm-scale sigmoidal beds of trough cross-stratified (S_t) and low angle cross-stratified (S_h) metasandstone occur in the lower part of this basal succession. Dm- to m-thick wave-ripple cross-laminated (S_r_w) (Fig. 3B) and current ripple cross-laminated metasandstone (S_r_c) beds overlay, and cm-scale intervals with climbing ripples can occur locally. These are commonly associated with SST in their upper bedding surface. The S_r facies is interbedded with cm- to dm- scale tabular and sigmoidal sets of fine- to medium-grained trough cross-stratified metasandstone (S_t).

The ~7 m-thick intermediate succession is also organized in a fining-upward package, where dm- to m-thick sigmoidal sets of trough cross-stratified metasandstone (S_t) are interbedded with equally thick tabular beds of cm-scale current ripple cross-laminated metasandstone (S_r_c) (Fig. 3C). Towards the top, a thick interval (ca. 3.5 m) of fine- to medium-grained, low angle cross-stratified metasandstone (S_h) dominates. This facies is organized in m-thick beds that are separated by mm- to cm-scale S_r_c which, as an example of the lower current ripples (Fig. 3D), also present SST in its plane beds.

In the upper 6-m-thick succession, wedge-shaped sets of medium-grained metasandstone with trough cross-stratification (S_t) dominates (Fig. 3E), commonly grading to fine-grained ripple cross-laminated metasandstone (S_r_c). Also, swalley

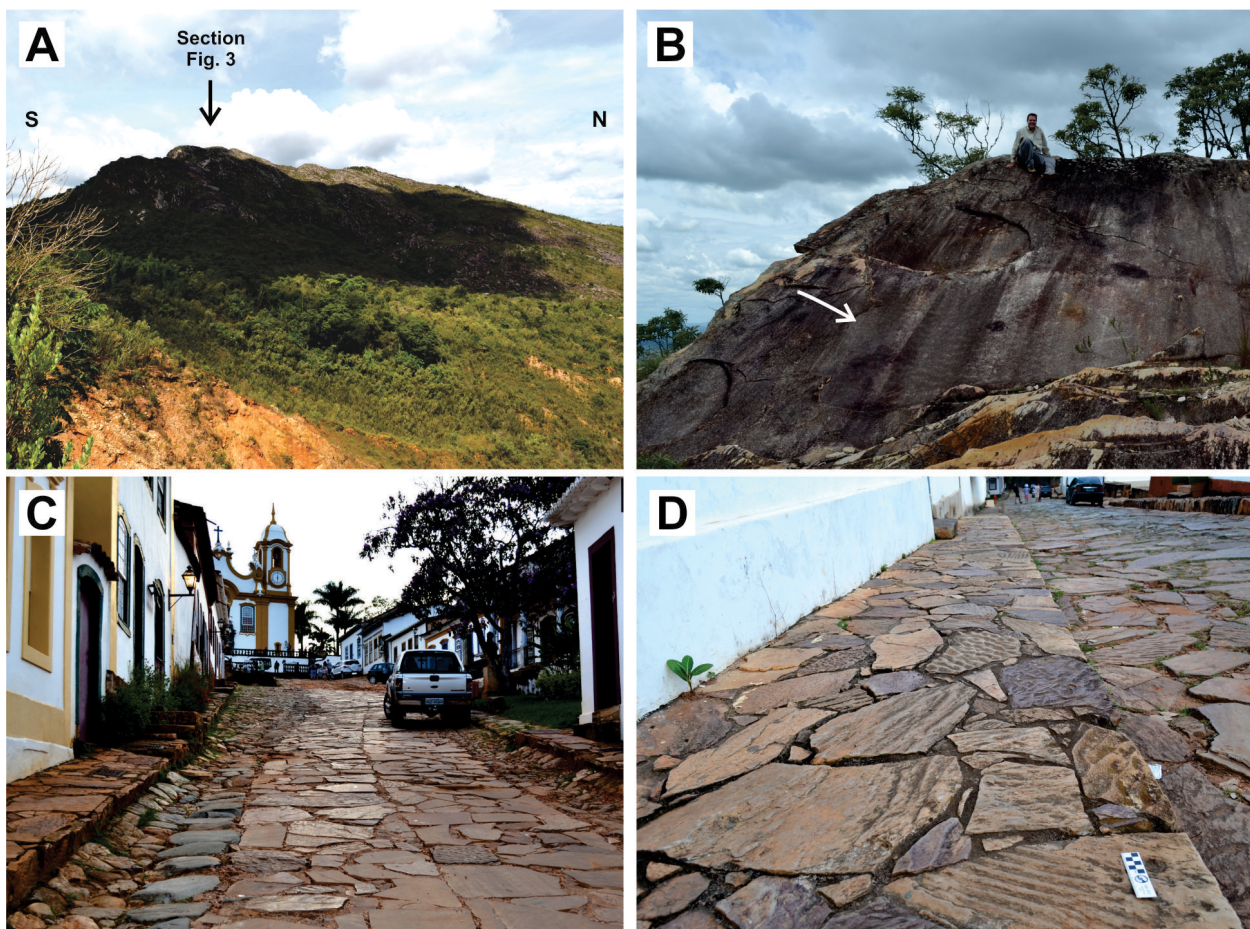
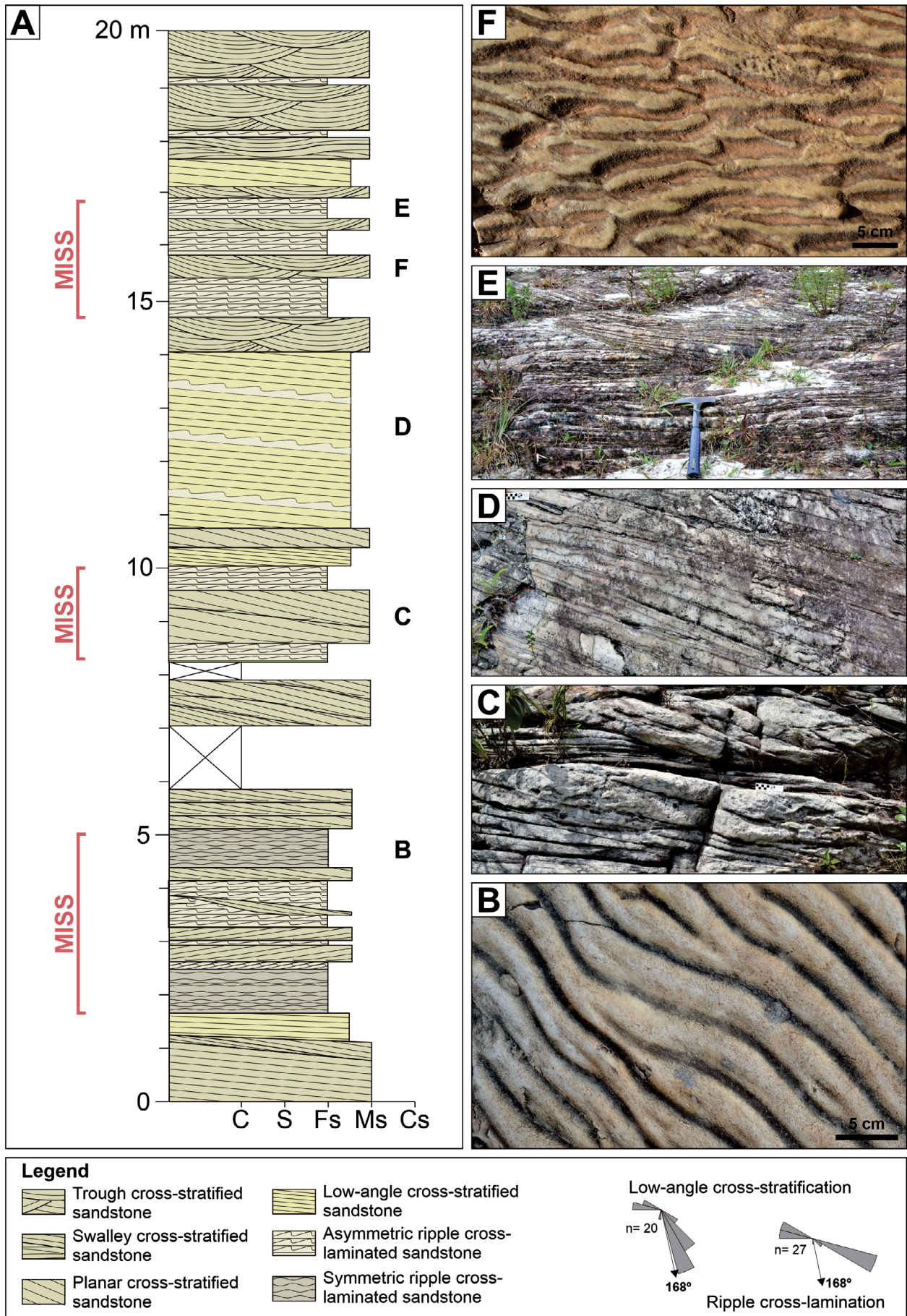


Figure 2. The paving stones of Tiradentes, SW of Brazil. (A) Panoramic view of a classic street in the historic town of Tiradentes, showing the natural, metasandstone-derived pavement. (B) View of the eastern part of the São José Ridge from the town of Prados. The location of the old quarry where the columnar section was acquired (Fig. 3) is pointed by a black arrow. (C) Detail of paving stones displaying several examples of well-preserved ripple marks. (D) General view of the old quarry where the metasandstone rock slabs were collected. Note the pronounced dip of the beds (~20/30).



C: clay; S: silt; Fs: fine sand; Ms: medium sand; Cs: coarse sand.

Figure 3. Stratigraphic constrain of the analyzed SST. (A) Columnar section, sedimentary facies of the Tiradentes Sequence shoreface deposits acquired in the old quarry, at the eastern part of the São José Ridge (see Fig. 1 for the precise location). (B) Fine metasandstone showing symmetric wave ripples. (C) Amalgamated tidal bars. (D) Low angle cross-stratified metasandstone with rippled laminae. (E) Wedge-shaped bed of trough cross-stratified metasandstone. (F) Asymmetric ripple laminated metasandstone.

cross-stratified metasandstone (Ss) is common, mainly associated with the lower part of the coarsening-upward successions. The thickness of St increases upwards, whereas Sr_c beds become thinner upwards. At this interval, SST are abundant in the upper planes of Sr_c (Fig. 3F).

The overall succession is characteristic of shallow marine settings, probably representing tide- to wave-dominated deposits subjected to storm-wave action. The lower, fining upward succession suggests deposition in a tidal setting, with the amalgamation of tidal bars (subtidal to lower intertidal) at the base and presence of fine-grained ripple cross-laminated facies at the top (upper intertidal) (according to Davis Jr. and Dalrymple 2012). The intermediate succession is characterized at the base by tidal bars (amalgamated St facies with sigmoidal geometry, Olariu *et al.* 2012) and at the top by beach facies (low-angle cross-stratified metasandstone produced by swash and backwash movements, Clifton 1969, Davis Jr. and Dalrymple 2012). Finally, the stacking pattern of the upper succession (coarser-grained and thicker beds towards the top) suggests a prograding wave-dominated cycle with local foreshore storm deposition (swalley). Paleocurrents measured in the low-angle cross-beds and ripple cross-laminated facies (Fig. 3) show persistent oscillatory wave movements in the NW-SE direction, indicating a paleoshore positioned in the NE-SW direction.

SEDIMENTARY SURFACE TEXTURES

The SST described in this study only occur in metasandstone from the uppermost succession of the Tiradentes Sequence. Despite the common presence of these structures in the rock exposure located in the eastern part of the São José Ridge (= old quarry, Figs. 2A and 2B), the most representative examples were observed in non-weathered rock slabs used for paving the historic streets of the town of Tiradentes (Figs. 2C and 2D). In total, 306 paving stones were analyzed, with nearly half

of them (148 samples, 48.4%) showing SST on the exposed bedding surface. Regardless of their modes of occurrence, all types of SST occur in fine to medium-grained ripple-cross laminated metasandstone (Figs. 2 and 3), partially or fully covering the bedding surface (Figs. 4 and 5). The identification of SST in the field revealed a preferred association with wave ripples (94 samples, 63.5%), and current ripples (54 samples, 36.5%). In other words, SST tend to occur by covering symmetric (wavy) and asymmetric (current) ripple marks deposited in the shallower waters of the depositional setting (Fig. 3A).

At the old quarry section, the SST are abundant and present in all three intervals described in the succession, associated with both wave and current ripple cross-laminations (see Fig. 3). These are particularly more abundant in the intermediate and upper intervals, where current ripples are more common than wave ripples. When observed in the outcrop, the regularity of individual beds of wavy ripple cross-laminated sandstone is also noteworthy, showing SST on the bedding surface. In some cases, almost all original depositional surfaces have evidence of SST in a frequency per area of about 1 structure/cm.

Three different patterns of SST were observed, herein named as Types 1, 2, and 3. The most frequent SST observed is characterized by shallow (mm-scale) grooves and crests, with elongated, straight, or sinuous morphology, similar to a wrinkle pattern (Type 1), which covers the troughs and ridges of ripple marks (Figs. 4A-4D). The second structure (Type 2) observed has an mm-scale pustular-shaped morphology. These pustular morphologies occur scattered or in dense accumulations above ripple marks or flat beddings (Fig. 4E). A third common structure (Type 3) in the samples analyzed is represented by cm-scale dome structures that display torus-shaped (Figs. 5A-5C) or elongated dome-shaped (Figs. 5D-5F) morphologies. Contrary to the other SST, these latter structures were not observed directly above ripples, but are always associated with the intervals where they occur (see Fig. 5).

Table 1 – Sedimentary facies from the Mesoproterozoic Tiradentes Sequence.

Code	Facies	Description	Depositional process
Sr	Ripple cross-laminated sandstone	Cm- to dm-thick tabular beds, with undulated base and top, of fine-grained sandstone. Meter-thick beds are composed of cm-scale ripples (symmetric and asymmetric) and rare supercritical climbing ripples.	Migration of ripple marks under lower flow regime produced by the action of unidirectional bottom currents (asymmetric) and fair-weather wave oscillations (symmetric). Supercritical climbing ripples are the product of increased deposition rate in relation to the tangential celerity (Allen 1982).
Sh	Low angle cross-stratified sandstone	0.5 to 2.5 m-thick tabular beds, with sharp base and top, of fine- to medium-grained sandstone presenting horizontal to low angle cross-stratification. This facies is usually related to Sr.	Attenuated bedform produced in the transition between the lower and upper flow regimes (Best and Bridge 1992) by the action of swash and backwash movements (Clifton 1969).
Sp	Planar cross-stratified sandstone	0.25 to 1.25 m-thick tabular beds, with sharp base and top, of medium-grained sandstone presenting planar cross-stratification.	Migration of subaqueous, two-dimensional dunes, under unidirectional lower flow regime (Allen 1963, Miall 2006).
St	Trough cross-stratified sandstone	0.25 to 1 m-thick beds with tabular, wedge-shaped, and sigmoidal morphology, of fine to medium-grained sandstone presenting trough cross-stratification.	Migration of subaqueous, three-dimensional dunes, under unidirectional lower flow regime (Allen 1963, Miall 2006).
Ss	Swalley cross-stratified sandstone	Dm-scale tabular beds, with sharp base and undulated top, of medium-grained sandstone presenting swalley cross-stratification with dm-scale amplitude and cm-scale height.	Generated by long-wave periods and moderate oscillatory velocities and very weak unidirectional flow, below fair-weather wave base and above storm wave base, under low aggradation rates (Dumas and Arnott 2006).

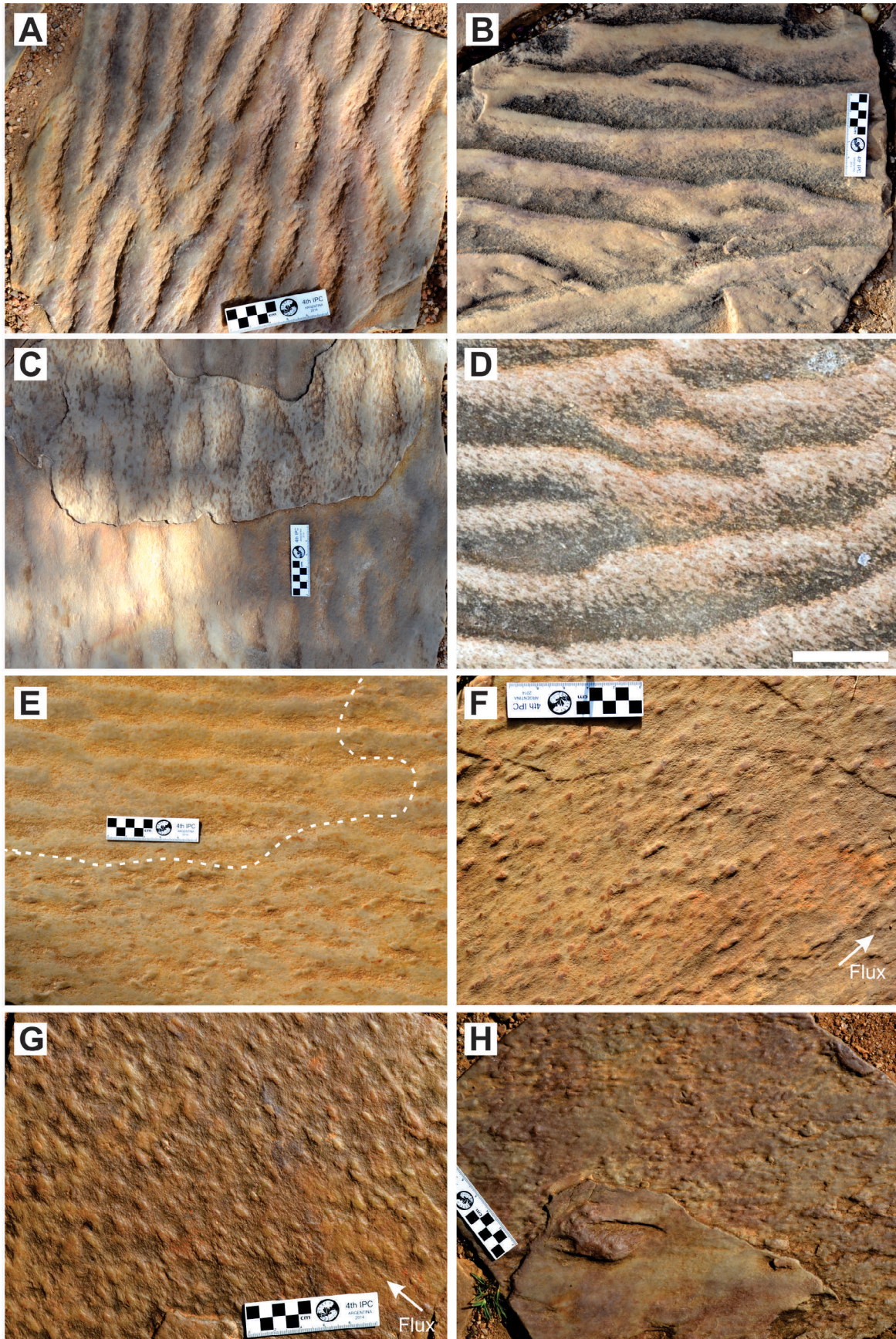


Figure 4. Honey-comb and pustular SST from the Tiradentes Sequence (Types 1 and 2, respectively). (A) Wave rippled surface entirely covered by honeycombed SST. (B) Current rippled metasandstone slab partially covered by honeycombed SST. (C) Current ripples partially covered by honeycombed SST. Note that the surface bearing SST is identical to the lower rippled surface. (D) Detail of rippled surface completely covered by honeycombed SST. (E) Partial covering of a rippled surface by small-scale pustular SST. The white dashed line represents the limit of the original microbial mat. Note that the pustular structures seemingly occur above the slightly rippled surface. (F-G) Detail of SST characterized by slightly aligned pustular structures (white arrow points to the paleoflow). (H) Irregular pustular structures without evident preferential orientation. The scale bar in D is 5 cm in length. All structures are preserved in positive epirelief, and the white arrow indicates the shear vector as the flow direction.

Wrinkle structures (Type 1) were observed fully or partially covering the current (asymmetric) or wave (symmetric) ripple marks in fine metasandstone (Figs. 4A-4D). Type 1 structures are more developed on the troughs of the rippled surface (Figs. 4C and 4D). Occasionally, the upper bed bearing honeycombed SST molds the lower rippled bed, displaying an identical rippled pattern (Fig. 4D). In detail, the honeycombed structures are discontinuous, elongated, and bifurcated forms with flat-topped crests separated by irregular and aligned troughs (Fig. 4D). In general, the size of individual alveolus/cavities varies between a minimum of 0.2 and a maximum of 10 mm. The width and length of crests never exceed 0.5 and 30 mm.

Pustular structures (Type 2) also occur above rippled or flat beddings (Figs. 4E-4H) and commonly show some degree of alignment (Fig. 4F and 4G), although surfaces with pustules without evident orientation also occur (Fig. 4H). Generally, the small pustules vary in size between 3 and 30 mm (Figs. 4F and 4H), and are preserved in positive epirelief, elevating less than 1 mm from the bedding plane. Hyporelief counterparts were rarely observed, showing a characteristic pitted texture, interpreted as the external molds of individual small pustules/nodules preserved as negative relief. The density in the area of pustular surfaces is usually between 1.5 and 2 individual pustules/cm², locally reaching 2-3 pustules/cm² forming local swarms (Sarkar *et al.* 2011). Some samples observed in petrographic slides reveal that the pustules/

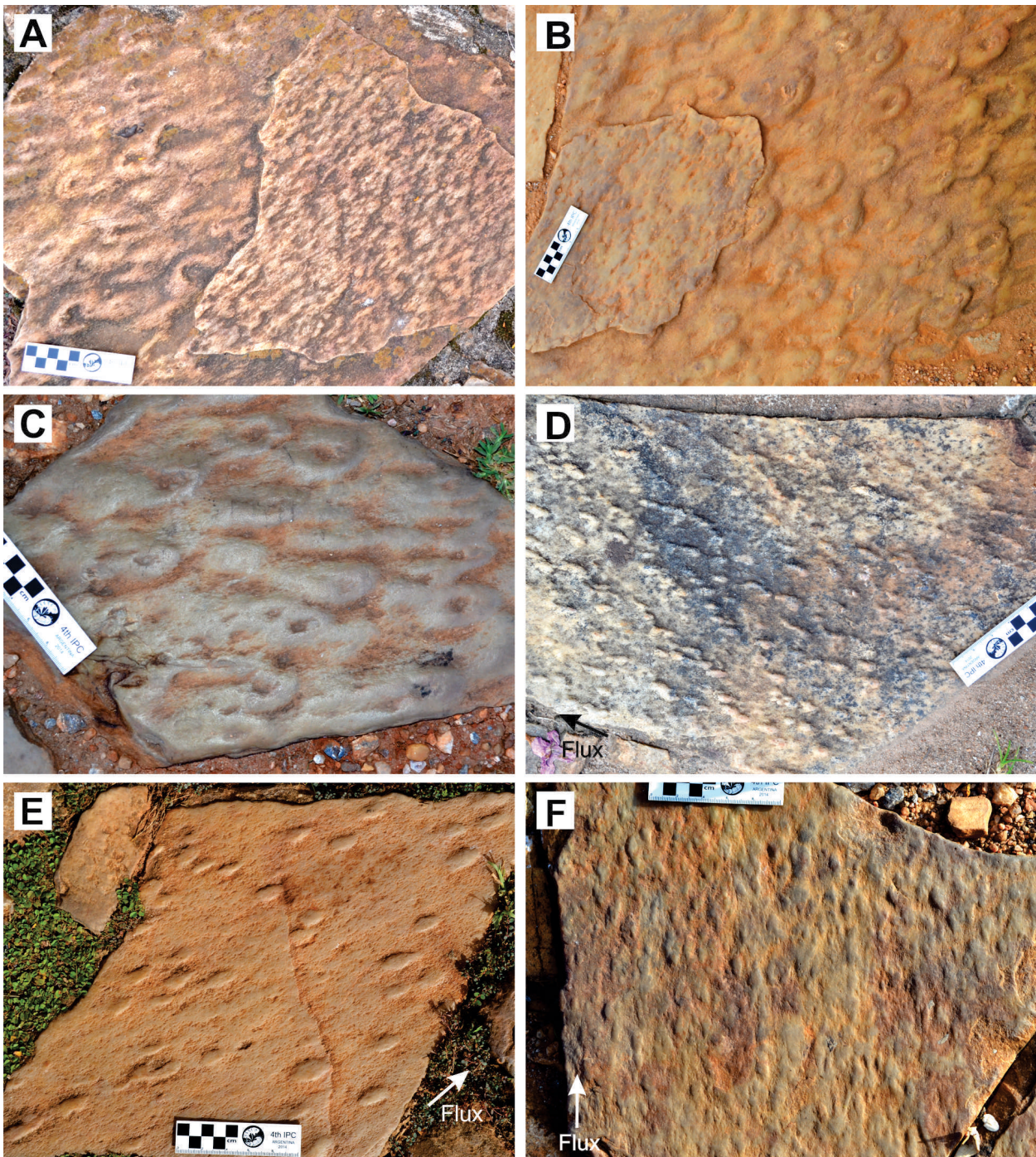


Figure 5. Domed structures from the Tiradentes Sequence, SW Brazil (Type 3). (A-C) Large-sized torus-shaped structures, characterized by raised borders and a depressed central region. These structures are partially covered by a surface bearing “Kinneyia-like” SST (A). (D-F) Aligned and elongated circular domed structures on flat bedding. All structures (A-F) are preserved in positive epirelief, except for E (negative hypolief).

nodules are locally covered by very-fine crystals of phyllosilicate (sericite; Fig. 6A). Cusped erosive forms have not been observed, but some samples show sediment accumulation in the leeward side of the pustules (Figs. 4E and 4F and 7).

The cm-scale dome structures (Type 3) occur in horizontally stratified or low-angle cross stratified beds associated with intervals rich in ripple cross-laminated metasandstone. They occur with two distinctive morphologies: positive epirelief discoidal structures defined by well-marked raised rims and a central depression, resembling a torus-shaped feature (Figs. 5A-5C), and positive epirelief and negative hyporelief small sediment pimples, or protrusions, forming a simple dome-shaped feature (Figs. 5D-5F). Discs are generally elongated (width/length ratio varies from 0.3 to 1.2, but most of the values are concentrated at 0.7), varying in length from 7.9 to 82.6 mm and in width from 4.7 to 66 mm (Fig. 8). Only a small number of structures ($n = 6$

of 160) show a near-circular geometry. When torus-shaped discs are present, their central depression is typically voided and their length varies from 2.4 to 52.9 mm and width varies from 1.2 to 35.4 mm, also showing an elongated shape (0.62 width/length ratio). Both torus- and dome-shaped discs are notably oriented according to a preferential direction (see Fig. 5). The density of the structures varies between 1.2 to 1.5 structures/cm², and structures occur scattered or in clusters according to the preferential orientation (Figs. 5A-5C). On non-weathered (i.e. fresh metasandstone slabs) bedding planes, it was possible to observe that the surface was covered by very thin sericite lamina, a situation also observed in the thin section (see Fig. 6B). When observed under the microscope, the sericite laminae are less than 0,01 mm thick and composed of individual sericite grains, suggesting that these were an originally laterally continuous layer of clay minerals later being affected by low-grade metamorphism.

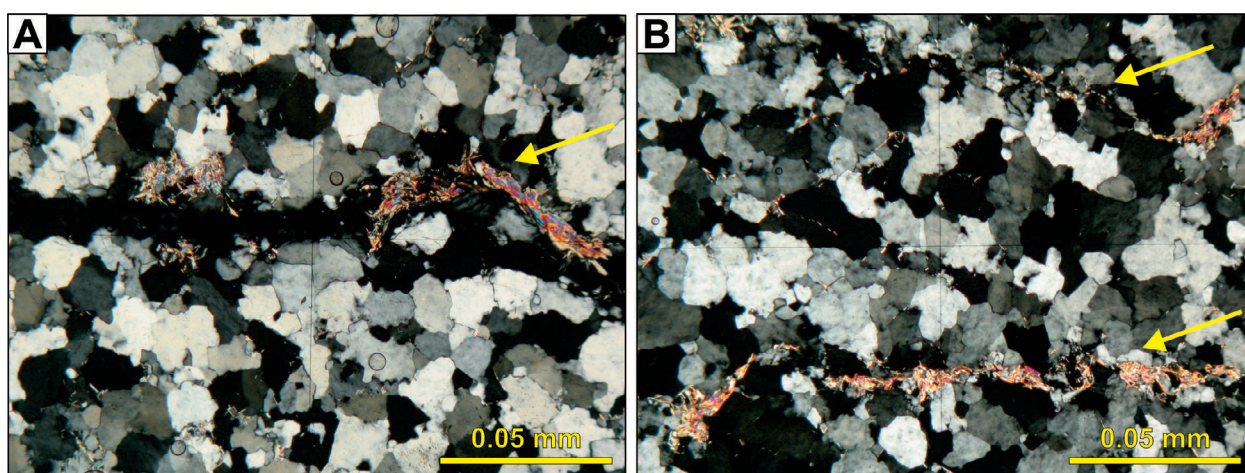


Figure 6. (A and B) Thin sections of metasandstone, showing phyllosilicate (sericite) (yellow arrows) covering the putative original depositional surface.

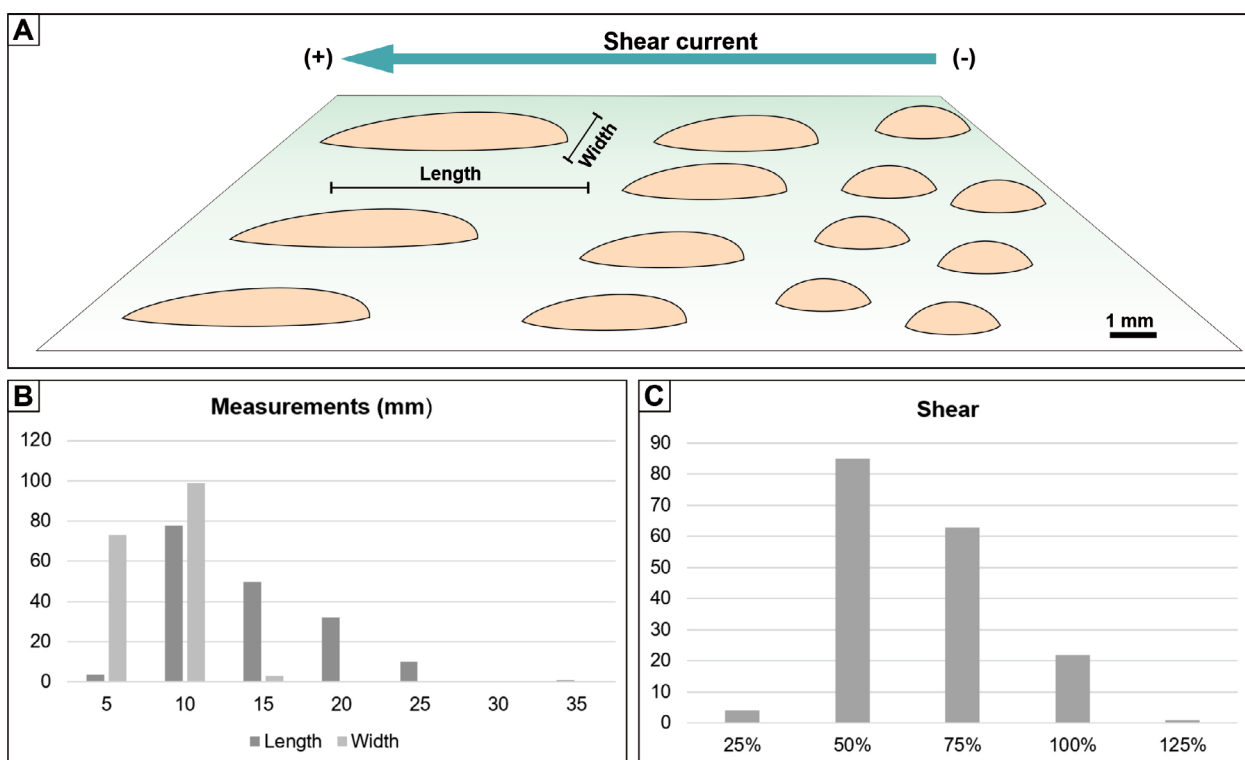


Figure 7 – Type 2 SST morphologies. (A) Model of formation of pustular structures. (B) Measurements of length and width. (C) Histogram showing normal distribution of the width/length ratios of pustular structures.

MICROBIAL ORIGIN OF THE SURFACE SEDIMENTARY TEXTURES

The structures (Types 1, 2, and 3) observed in the metasandstone from the upper part of the Tiradentes Sequence are extremely common and occur in association, commonly in overlapping centimeter-thick beds (see Figs. 4E and 5A). The high frequency of superposed surfaces bearing SST observed in outcrops is another striking feature, suggesting that the original depositional surface almost always presents some type of structure. The most common SST observed is Type 1, followed by Types 2 and 3.

Type 1 structures have a typical honeycombed arrangement and are similar to those classified as honeycombed or “Kinneyia”-like structures, such as those exemplified by Hagadorn and Bottjer (1997), Bottjer and Hagadorn (2007), Porada and Bouougri (2007), and Porada *et al.* (2008). In general, “Kinneyia”-like structures are small-sized forms, from 3-30 mm of wavelength (Herminghaus *et al.* 2016), and the honeycombed pattern usually has millimetric alveolus/cavities. It is important to note that all Type 1 structure samples were described in non-weathered rock slabs with no evidence of granular disintegration, micro-delamination, pores, and alveoli (Smith *et al.* 2005). Thus, the honeycombed pattern probably represents the original organic surface and was not produced by post-depositional alteration or weathering.

Although the lower size class overlaps, the Type 1 structures described herein are slightly bigger than others from Neoproterozoic and Phanerozoic successions (Bouougri and Porada 2002, Porada and Bouougri 2007, Porada *et al.* 2008, Davies *et al.* 2016). However, the size and shape are compatible with other Mesoproterozoic examples (Noffke and Chafetz

2011, Tang *et al.* 2011). Despite some recent controversy (see discussion in Davies *et al.* 2016), the origin of “Kinneyia” is frequently assigned to an organic influence to some degree, either as lithified organic surfaces (Noffke *et al.* 2001), gas bubbles produced and trapped beneath microbial mats (Hagadorn and Bottjer 1999), or as small-scale load casts formed beneath beds of microbial mats (Noffke *et al.* 2002, Davies *et al.* 2016). In any case, experimental studies were able to reproduce wrinkled structures remarkably similar to a “Kinneyia” pattern, suggesting that the development of this class of structures is influenced by the presence of microbial mats and aggregates supporting its organic affinity (Thomas *et al.* 2013, Mariotti *et al.* 2014, Herminghaus *et al.* 2016). Considering this, the presence of thin beds bearing honeycombed structures developed over structures from the bed immediately below (Fig. 4C) indicates that the ripple marks were covered by sediments on which Type 1 structures developed. In other words, this occurrence style putatively suggests the preservation of the original organic surface over the previously deposited rippled surface. In this way, this type of structure is considered comparable to the “transparent wrinkle structures” described by Noffke (2000, 2009) and Noffke *et al.* (2002).

The pustules swarms observed at the rippled or flat bedding from the Tiradentes Sequence are strikingly similar in shape and size to structures interpreted as inverted flutes, or setulfs, as defined by Friedman and Sanders (1974). These small (mm-scale) pustular and elongated bedforms are deposited as the result of high-speed unidirectional subaqueous currents or winds (Sarkar *et al.* 2011), upon an exposed damp substrate of fine sand, where the presence of exceedingly small obstacles (most likely unfossilized organic debris) and the

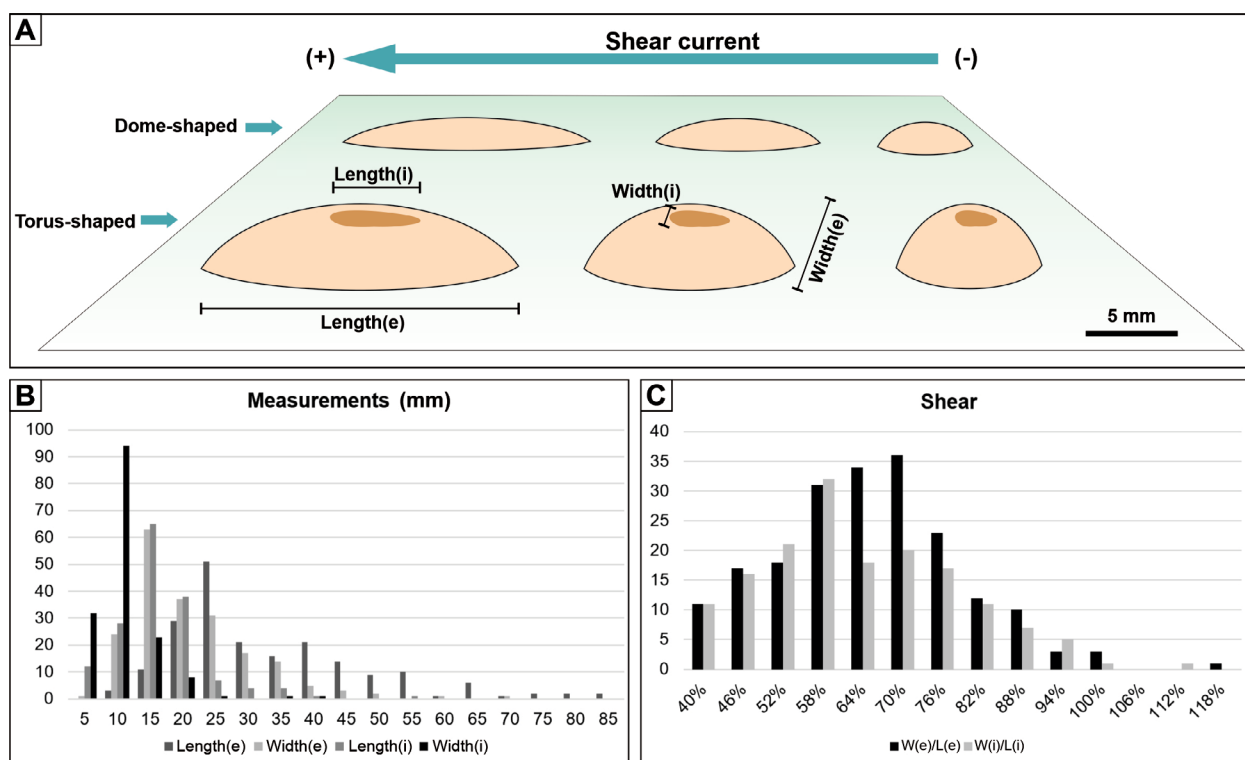


Figure 8 – Type 3 SST morphologies. (A) Model of elongated dome- and torus-shaped disc SST formation. (B) Measurements of external and internal length and width of discs. (C) Histogram showing normal distribution (dotted orange line) of the width/length ratios of external and internal discs.

enhanced cohesion of the wet sediment induce the accumulation of material leeward the miniature obstacles (Sarkar *et al.* 2011). According to Sarkar *et al.* (2011), the positive, small-scale elevations formed in exposed or very shallow coastal settings (Bottjer and Hagadorn 2007) have very low preservation potential and were exclusively preserved by sealing of the substrate promoted by the covering of microbial mats. Thus, this organic protection was responsible for stabilizing the loose sand protecting it and allowing the fossilization of this delicate structure in very shallow (inter to supratidal) environments. It is important to note that in some cases the distribution of the pustule swarms also resembles patchy ripples described by Sarkar *et al.* (2014) for Neoproterozoic intertidal sandstone from the Jodhpur Group, India. In both Indian and Brazilian occurrences, the presence of ripples just under storm or upper-flow regime beds without being covered by a mud lamina is suggestive of preservation by microbial mats (Sarkar *et al.* 2014). Despite a possible sampling bias (Davies *et al.* 2016), the massive occurrence of setulfs and patchy ripples in the Proterozoic and early Paleozoic probably reflects the abundance of biofilm mats at this time interval (Sarkar *et al.* 2011).

Type 3 SST have a dome shape, and although circular morphologies are present, most of the structures are elongated (Figs. 5B-5D and 8A). Also, most of the observed structures have a torus-shaped morphology (160 from 199; see Supplementary Materials Section). The association of these morphologies with upper-flow regime structures (planar cross-stratified sandstone, Sp) in the presence of sericite-rich laminae is noteworthy. Interestingly, the general orientation of these structures (and also of Type 2 structures) has different directions in distinct overlapping layers, which allows their alignment by tectonic stretching to be ruled out. Similar structures have been previously interpreted as fluid-escape (*Intrites*-like structure, *sensu* Menon *et al.* 2015) and gas domes (Noffke 2010). However, *Intrites*-like structures are described as millimetric discoidal mounds commonly preserved in hyporelief, unlike the often centimeter-scale torus-shaped features we present, which occur at the top of sedimentary beds. In any case, the morphology of the torus-shaped structures is coherent with what is expected of a fluid-escape feature (e.g., gas-domes or sand-volcanoes) with a collapsed central region (Sarkar *et al.* 2014, Taj *et al.* 2014, Menon *et al.* 2015). During growth and decay, gases produced under mats by the metabolic activity of microbes may accumulate and migrate upwards, building up underneath an impervious microbially stabilized layer resulting in a dome-like structure (Sarkar *et al.* 2014, Taj *et al.* 2014, Tu *et al.* 2016, Menon *et al.* 2015, 2016). A depressed central region in these discoidal mounds is most likely a response to the relaxation of the pressure generated by the upward movement of fluids, which leads to a partial collapse of the structure before burial (Noffke 2010, Menon *et al.* 2016). As cross-section observations were not performed in these structures, no internal features, such as a central fluid conduit or microbial lamination, could be observed in these features. From the morphological perspective, a striking elongation,

oriented to a preferential orientation was observed in most of the Type 3 structures measured. Preferential elongation parallel to the paleocurrents suggests that circular domed structures may have formed under more quiet conditions and were sheared afterward by strong currents, which is seen by the normal distribution of the width/length ratios of both external and internal discoidal features (see Fig. 8).

Selected samples of metasandstone showing ripple cross-lamination associated with SST were petrographically characterized as quartz-sandstone with incipient metamorphic recrystallization. The framework is composed of quartz grains (ca. 90%) and muscovite (sericite; ca. 5%) and opaque minerals (ca. 5%). The micas occur in thin and irregular laminae (Figs. 6A and 6B) above the sutured and aligned quartz grains showing well-marked segregation of the well-sorted grains, highlighting foresets of the ripples. The distribution of the phyllosilicate grains sandwiched by ripple cross-laminations is noteworthy. This condition could be achieved by two main processes: deposition of mica in the troughs of ripple marks during standing waters; or stabilization of ripple marks by microbial biofilms, also during standing water conditions, followed by trapping of phyllosilicate (clay-minerals or sericite, Noffke *et al.* 2001). Due to the association of ripples with honeycombed, pustular, and elongated dome/torus surface marks, and considering the low-grade metamorphism in the area, it is suggested that micas were originally trapped by the mucilaginous biofilms, and thereby are interpreted as sinusoidal structures (*sensu* Noffke 2010). This condition suggests that biofilms influenced the development of SST upon ripples in two distinct ways (i.e., biostabilization and grain binding).

The classification of the analyzed structures as probably biotic in origin is grounded by several lines of evidence, such as:

- all structures (n = 148) correspond to original SST covering rippled or flat beddings;
- the pustular, nodular, honey-comb, and dome structures are comparable to modern and ancient examples described as MISS (Davies *et al.* 2016);
- several samples analyzed (especially pustular and dome structures) have some degree of alignment, probably reflecting deformation by the action of currents during deposition (i.e., reflect hydrodynamic conditions during deposition, Davies *et al.* 2016);
- the petrographic analysis reveals the presence of thin lamina constituted by sericite grains covering the original bedforms. As previously explained, these lamina are possibly not the product of weathering and is interpreted as the original cover of mats by adhered fine-grained sediments;
- textural evidence of sediment stabilization revealed by the segregation and orientation of quartz grains (Figs. 6A-6B).

Another important feature to attest to the biotic origin of MISS is the presence of preserved organic matter (Davies *et al.* 2016). However, depositional characteristics (deposition by high-energy processes in shoreface to offshore transition conditions) and the presence of very low-grade metamorphism virtually preclude the preservation of organic fraction.

THE IMPORTANCE OF MISS IN THE PRESERVATION OF SEDIMENTARY STRUCTURES AND SEDIMENT DISPERSION

Over the last decades, several works demonstrate that the preservation potential of delicate sedimentary structures such as ripples, tool, and flute marks are significantly increased by: events of rapid burial; immediate cover by mud/silt particles; absence of bioturbation; and presence of microbial/microalgal EPS covering (Deckere *et al.* 2001, Noffke *et al.* 2001, Friend *et al.* 2008, Noffke 2010, Davies *et al.* 2016, Cuadrado and Pan 2018, Tarhan 2018, Cuadrado 2020). In addition to the rapid burial and the cohesiveness that mud drapes promote on the marine substrate, the effect of bioturbation and organic protection in the preservation of sedimentary structures is striking (Tarhan 2018). In the first case, sediment mixing by infaunal organisms results in a substantially decreased fluid content and cohesiveness of the sediment obliterating the depositional framework, including sedimentary structures (Tarhan 2018). In the case of sole marks, the influence of bioturbation in their preservation is so significant that a sharp decline is observed in the record of these structures in the Phanerozoic following a progressive increase in the rates of sediment mixing by burrowing animals (Tarhan 2018). In this sense, the absence of significant bioturbation throughout almost the entire Precambrian may be pointed out as a major contributor to the abundance of preserved sedimentary structures (Dalrymple 2011), which is also coincident with the predominance of microbial forms at that time (Gehling 1999, Seilacher 1999, Bottjer *et al.* 2000, Mángano and Buatois 2014).

Despite those different interpretations regarding the mechanisms of SST formation (see Davies *et al.* 2016 for a complete compilation), several studies point to the influence of microbial communities in the origin of most of these structures (Dade *et al.* 1992, Hagadorn and Bottjer 1999, Noffke *et al.* 2001, 2002, Friend *et al.* 2008, Thomas *et al.* 2013, Mariotti *et al.* 2014, Baas *et al.* 2019, Cuadrado 2020). When present, biofilms and microbial mats are important to stabilize the substrate against erosion by currents or small-scale waves in shallow marine environments or even in Precambrian and early Phanerozoic eolian sediments (Noffke *et al.* 1996, 2001, Porada and Bouougri 2007, Callow and Brasier 2009, Tarhan 2018, Basilici *et al.* 2020, Cuadrado 2020). The presence of organic extracellular polymeric substances (EPS) covering the substrate directly influences the cohesiveness of sediment and its stability (Tolhurst *et al.* 2002), drastically reducing bed roughness, bottom stress, and bed erodibility (Friend *et al.* 2008). When the exposed substrate is covered by a mat or biofilm during a microbial bloom, the bedform is stabilized by the EPS and the movement tends to cease (Friend *et al.* 2008, Cuadrado 2020). With the vertical growth of the microbial colony, bed roughness decreases, reducing shearing produced by waves/currents and consequently the erosion of substrate (Friend *et al.* 2008). This process clearly increases the potential preservation of delicate bedforms (Friend *et al.* 2008), also allowing plastic deformation by current shearing, like Type 2 and Type 3 structures studied here (Figs. 4F and 4G and 5D-5F).

MISS are biogenic structures known in the geological record since the Paleo-Archean (Noffke *et al.* 2003, 2006). Notably, the presence of MISS is faciological and environmentally dependent (Noffke *et al.* 2006, Bayet-Goll and Daraei 2020, Sarkar *et al.* 2020). During the Precambrian, MISS are recorded mostly on paralic to shallow marine environments (Davies *et al.* 2016) associated mostly with siliciclastic facies (Noffke *et al.* 2003, 2006, Porada and Bouougri 2007, Basilici *et al.* 2020, Sarkar *et al.* 2020). The observation of modern tidal flats subjected to seasonal storm events shows that the flow energy in a given sedimentary environment plays a significant role in the mat and bedform morphology (Cuadrado 2020). In general, lower energy settings are associated with planar laminations, while higher energy deposits are related to 3D ripples and associated erosional MISS (Baas *et al.* 2019, Cuadrado 2020). The latter condition is expected to occur in a narrow strip between sandy tidal channels and muddy tidal flats where strong currents winnow the clay and EPS, and help preserve 3D morphologies (Baas *et al.* 2019).

The presence of planar lamination associated with collapsed gas domes, ripples, and planar laminated beds with sheared pustular MISS, and ripple marks associated with wrinkled surfaces, in the investigated interval, suggests deposition under changing energy conditions. The overall depositional pattern, from tide to wave-dominated settings towards the top of the section and the presence of distinct MISS associated with the well-preserved bedforms also points to such variable energies with implications in the potential preservation of these surficial structures. While gas domes and pustules are observed in higher density clusters in the lower tide-dominated interval, wrinkle marks are mainly observed in the upper wave-dominated beds. Although our data do not allow the observation of an evident relationship between the stratigraphic abundance of MISS and bedform preservation, the fact that mud-silt drapes and the number of bedforms covered by surface textures are absent is striking. Furthermore, most of the observed MISS are associated with evidence of strong flow velocities, such as those responsible for the deposition of 3D ripples. Also, planar-laminated sandstone with preservation of thicker mats is present, suggesting lower flow velocities, which were further sheared by subsequent strong currents, resulting in elongated setulfs and sheared gas domes. The grain size of these bedforms varies between fine to medium sand, which could be misinterpreted as a product of deposition in relatively low-energy environments. However, as pointed out before, the presence of biofilms changes the response of sediments to high flow energies; therefore, the energy is not directly reflected in grain size in such conditions (see discussion in Cuadrado 2020).

CONCLUSIONS

MISS are widespread in the Mesoproterozoic Tiradentes Formation of the São João Del Rei Basin, São Francisco Craton, Brazil. The identified structures (Types 1, 2, and 3) fulfill the key features attesting to their biological origin, including 3D morphology, patterns of deformation, evidence of original biostabilization, and great similarity

with modern and fossil examples. The specific association of ripple marks with wrinkled surfaces and ripple and planar laminated beds with domes and pustular structures indicate deposition under variable flow conditions. Therefore, our data consistently show that changes in the morphology of the MISS studied are likely derived from environmental controls on their morphogenesis and environmental distribution. Finally, in this studied case, the presence of biofilms directly conditioned the preservation of bedforms acting as a protective cover against erosion and transport by currents and waves. Thus, they are of key importance for bedform deposition and preservation in shallow marine siliciclastic environments. Considering previous reports and proposed ages for the unit, these are the oldest known MISS in South

America Precambrian successions. The profusion of sedimentary surfaces presenting MISS and preserved bedding structures indicate that the microbial benthic communities were abundant in the shallow sea that occupied this part of the São Francisco Craton during the Mesoproterozoic Era.

ACKNOWLEDGMENTS

The authors thank CNPq (Grant 301294/2018-6) for funding and IEF, Prados (Instituto Estadual de Florestas, Casa da Serra) for logistic support during the fieldwork. This work was made possible with the institutional support of Universidade Estadual Paulista "Júlio de Mesquita Filho". L.V.W. and M.G.S. are fellows of CNPq.

ARTICLE INFORMATION

Manuscript ID: 20200034. Received on: 05/05/2021. Approved on: 09/27/2021.

L.W.: conceptualization, fieldwork, formal analysis, funding acquisition, investigation, methodology, writing, review; F.V.: formal analysis, investigation, writing, review; F.Q.: fieldwork, formal analysis, writing, review; L.L.: formal analysis, writing, review; F.B.: fieldwork; formal analysis; M.S.: formal analysis, writing, review.

Competing interests: The authors declare no competing interests.

REFERENCES

- Allen J.R.L. 1963. Henry Clifton Sorby and the sedimentary structures of sands and sandstones in relation to flow conditions. *Geologie en Mijnbouw*, **42**:223-228.
- Allen J.R.L. 1982. Climbing ripples and dunes and their cross-stratification patterns. In: Allen J.R.L. (Ed.). *Sedimentary Structures: their character and physical basis*. Amsterdam: Elsevier, p. 345-382.
- Awramik SM., Sprinkle J. 1999. Proterozoic stromatolites: the first marine evolutionary biota. *Historical Biology*, **13**(4):241-253. <https://doi.org/10.1080/08912969909386584>
- Baas J.H., Baker M.L., Malarkey J., Baas S.J., Manning A.J., Hope J.A., Peakall F., Lichtman I.A., Ye L., Davies A.G., Parsons D.R., Paterson D.M., Thorne P.D. 2019. Integrating field and laboratory approaches for ripple development in mixed sand-clay-EPS. *Sedimentology*, **66**(7):2749-2768. <https://doi.org/10.1111/sed.12611>
- Basili G., Soares M.V.T., Mountney N.P., Colombera L. 2020. Microbial influence on the accumulation of Precambrian aeolian deposits (Neoproterozoic, Venkatpur Sandstone Formation, Southern India). *Precambrian Research*, **347**:105854. <https://doi.org/10.1016/j.precamres.2020.105854>
- Bayet-Goll A., Daraei M. 2020. Palaeoecological, sedimentological and stratigraphic insights into microbially induced sedimentary structures of the lower Cambrian successions of Iran. *Sedimentology*, **67**(6):3199-3235. <https://doi.org/10.1111/sed.12745>
- Best J., Bridge J. 1992. The morphology and dynamics of low amplitude bedwaves upon upper stage plane beds and the preservation of planar laminae. *Sedimentology*, **39**:737-752. <https://doi.org/10.1111/j.1365-3091.1992.tb02150.x>
- Bottjer D., Hagadorn J.W. 2007. Mat features in sandstones. In: Schieber J., Bose P.K., Eriksson P.G., Banerjee S., Sarkar S., Altermann W., Catuneanu O. (Eds.). *Atlas of Microbial Mat Features Preserved within Siliciclastic Rock Record*. Atlases in Geoscience, 2, Amsterdam: Elsevier, p. 53-71.
- Bottjer D., Hagadorn J.W., Dornbos S.Q. 2000. The Cambrian Substrate Revolution. *GSA Today*, **10**:1-8.
- Bouougri E., Porada H. 2002. Mat-related sedimentary structures in Neoproterozoic peritidal passive margin deposits of the West African Craton (Anti-Atlas, Morocco). *Sedimentary Geology*, **153**(3-4):85-106. [https://doi.org/10.1016/S0037-0738\(02\)00103-3](https://doi.org/10.1016/S0037-0738(02)00103-3)
- Burne R.V., Moore L.S. 1987. Microbialites: Organosedimentary deposits of benthic microbial communities. *Palaios*, **2**(3):241-254. <https://doi.org/10.2307/3514674>
- Callow R.H.T., Brasier M.D. 2009. Remarkable preservation of microbial mats in Neoproterozoic siliciclastic settings: implications for Ediacaran taphonomic models. *Earth-Science Reviews*, **96**(3):207-219. <https://doi.org/10.1016/j.earscirev.2009.07.002>
- Clifton H.E. 1969. Beach lamination: nature and origin. *Marine Geology*, **7**(6):553-559. [https://doi.org/10.1016/0025-3227\(69\)90023-1](https://doi.org/10.1016/0025-3227(69)90023-1)
- Cuadrado D.G. 2020. Geobiological model of ripple genesis and preservation in a heterolithic sedimentary sequence for a supratidal area. *Sedimentology*, **67**(5):2747-2763. <https://doi.org/10.1111/sed.12718>
- Cuadrado D.G., Pan J. 2018. Field observations on the evolution of reticulate patterns in microbial mats in a modern siliciclastic coastal environment. *Journal of Sedimentary Research*, **88**(1):24-37. <https://doi.org/10.2110/jsr.2017.79>
- Dade W.B., Nowell A.R.M., Jumars P.A. 1992. Predicting erosion resistance of muds. *Marine Geology*, **105**(1-4):285-297. [https://doi.org/10.1016/0025-3227\(92\)90194-M](https://doi.org/10.1016/0025-3227(92)90194-M)
- Dalrymple R.W. 2011. Introduction to siliciclastic facies models. In: James N.P., Dalrymple R.W. (Eds.). *Facies Models 4*. *GEOtext 6*, p. 59-72.
- Davey M.E., O'Toole G.A. 2000. Microbial biofilms: From ecology to molecular genetics. *Microbiology and Molecular Biology Reviews*, **64**(4):847-867. <https://doi.org/10.1128/mmb.64.4.847-867.2000>
- Davies N.S., Liu A.G., Gibling M.R., Miller R.F. 2016. Resolving MISS conceptions and misconceptions: A geological approach to sedimentary surface textures generated by microbial and abiotic processes. *Earth-Science Reviews*, **154**:210-246. <https://doi.org/10.1016/j.earscirev.2016.01.005>
- Davis Jr., R.A., Dalrymple R.W. 2012. *Principles of Tidal Sedimentology*. London: Springer Dordrecht Heidelberg, 621 p.

- Decho A.W. 2000. Microbial biofilms in intertidal systems: an overview. *Continental Shelf Research*, **20**(10-11):1257-1273. [https://doi.org/10.1016/S0278-4343\(00\)00022-4](https://doi.org/10.1016/S0278-4343(00)00022-4)
- Deckere E.M.G.T., Tolhurst T.J., Brouwer J.F.C. 2001. Destabilization of cohesive intertidal sediments by infauna. *Estuarine, Coastal and Shelf Science*, **53**(5):665-669. <https://doi.org/10.1006/ecss.2001.0811>
- Dumas S., Arnott R.W.C. 2006. Origin of hummocky and swaley cross-stratification – The controlling influence of unidirectional current strength and aggradation rate. *Geology*, **34**(12):1073-1076. <https://doi.org/10.1130/G22930A.1>
- Folk R.L. 1980. *Petrology of sedimentary rocks*. Austin: Hemphill, 182 p.
- Friedman G.M., Sanders, J.E. 1974. Positive-relief bedforms on modern tidal flat that resemble molds of flutes and grooves; implications for geopetal criteria and for origin and classification of bedforms. *Journal of Sedimentary Research*, **44**(1):181-189. <https://doi.org/10.1306/74D729B9-2B21-11D7-8648000102C1865D>
- Friend P.L., Lucas C.H., Holligan P.M., Collins M.B. 2008. Microalgal mediation of ripple mobility. *Geobiology*, **6**(1):70-82. <https://doi.org/10.1111/j.1472-4669.2007.00108.x>
- Gehling J.G. 1999. Microbial mats in the terminal Proterozoic siliciclastics: Ediacaran death masks. *Palaio*, **14**(1):40-57. <https://doi.org/10.2307/3515360>
- Hagadorn J.W., Bottjer D.J. 1997. Wrinkle structures: Microbially mediated sedimentary structures common in subtidal siliciclastic settings at the Proterozoic-Phanerozoic transition. *Geology*, **25**(11):1047-1050. [https://doi.org/10.1130/0091-7613\(1997\)025%3C1047:WSMSS%3E2.3.CO;2](https://doi.org/10.1130/0091-7613(1997)025%3C1047:WSMSS%3E2.3.CO;2)
- Hagadorn J.W., Bottjer D.J. 1999. Restriction of a late Neoproterozoic biotope: suspect-microbial structures and trace fossils at the Vendian-Cambrian transition. *Palaio*, **14**(1):73-85. <https://doi.org/10.2307/3515362>
- Herminghaus S., Thomas K.R., Aliaskariso H., Porada H., Goehring L. 2016. Kinneyia: a flow-induced anisotropic fossil pattern from ancient microbial mats. *Frontiers in Materials*, **3**:30. <https://doi.org/10.3389/fmats.2016.00030>
- Kumar S., Ahmad S. 2014. Microbially induced sedimentary structures (MISS) from the Ediacaran Jodhpur Sandstone, Marwar Supergroup, western Rajasthan. *Journal of Asian Earth Sciences*, **91**:352-361. <https://doi.org/10.1016/j.jseas.2014.01.009>
- Mángano M.G., Buatois L.A. 2014. Decoupling of body-plan diversification and ecological structuring during the Ediacaran-Cambrian transition: evolutionary and geobiological feedbacks. *Proceedings of the Royal Society B: Biological Sciences*, **281**(1780):20140038. <https://doi.org/10.1098/rspb.2014.0038>
- Mariotti G., Pruss S.B., Perron J.T., Bosak T. 2014. Microbial shaping of sedimentary wrinkle structures. *Nature Geoscience*, **7**:736-740. <https://doi.org/10.1038/ngeo2229>
- Martins-Neto M.A. 2000. Tectonics and sedimentation in a Paleo/Mesoproterozoic rift-sag basin (Espinhaço basin, southeastern Brazil). *Precambrian Research*, **103**(3-4):147-173. [https://doi.org/10.1016/S0301-9268\(00\)00080-2](https://doi.org/10.1016/S0301-9268(00)00080-2)
- McIlroy D., Walter M.R. 1997. A reconsideration of the biogenicity of *Arumberia banksi* Glaessner and Walter. *Alcheringa*, **21**(1):79-80. <https://doi.org/10.1080/03115519708619187>
- Menon L.R., McIlroy D., Brasier M.D. 2016. 'Intrites' from the Ediacaran Longmyndian Supergroup, UK: a new form of microbially-induced sedimentary structure (MISS). *Geological Society of London Special Publications*, **448**:271-283. <https://doi.org/10.1144/SP448.12>
- Menon L.R., McIlroy D., Liu A., Brasier M.D. 2015. The dynamic influence of microbial mats on sediments: fluid escape and pseudofossil formation in the Ediacaran Longmyndian Supergroup, UK. *Journal of the Geological Society*, **173**:177-185. <https://doi.org/10.1144/jgs2015-036>
- Miall A. 2006. *The geology of fluvial deposits: sedimentary facies, basin analysis, and petroleum geology*. Berlin: Springer, 582 p.
- Neumann A., Gebelein C., Scoffin T. 1970. The composition, structure and erodibility of subtidal mats, Abaco, Bahamas. *Journal of Sedimentary Petrology*, **40**(1):274-297. <https://doi.org/10.1306/74D71F2D-2B21-11D7-8648000102C1865D>
- Noffke N. 2000. Extensive microbial mats and their influences on the erosional and depositional dynamics of a siliciclastic cold water environment (Lower Arenigian, Montagne Noire, France). *Sedimentary Geology*, **136**(3-4):207-215. [https://doi.org/10.1016/S0037-0738\(00\)00098-1](https://doi.org/10.1016/S0037-0738(00)00098-1)
- Noffke N. 2009. The criteria for the biogenicity of microbially induced sedimentary structures (MISS) in Archean and younger, sandy deposits. *Earth-Science Reviews*, **96**(3):173-180. <https://doi.org/10.1016/j.earscirev.2008.08.002>
- Noffke N. 2010. *Geobiology: microbial mats in sandy deposits from the Archean Era to today*. Berlin: Springer, 194 p.
- Noffke N., 2018. Comment on the paper by Davies et al. "Resolving MISS conceptions and misconceptions: A geological approach to sedimentary surface textures generated by microbial and abiotic processes". *Earth-Science Reviews*, **176**:373-383. <https://doi.org/10.1016/j.earscirev.2017.11.021>
- Noffke N., Gerdes G., Klenke T., Krumbein W.E. 1996. Microbially induced sedimentary structures - Examples from modern sediments of siliciclastic tidal flats. *Zentralblatt Geologie und Paläontologie*, **1**:307-316.
- Noffke N., Gerdes G., Klenke T., Krubein W.E. 2001. Microbially induced sedimentary structures - a new category within the classification of primary sedimentary structures: perspectives. *Journal of Sedimentary Research*, **71**(5):649-656. <https://doi.org/10.1306/2DC4095D-0E47-11D7-8643000102C1865D>
- Noffke N., Hazen R., Nhlenko N. 2003. Earth's earliest microbial mats in a siliciclastic marine environment (2.9 Ga Mozaan Group, South Africa). *Geology*, **31**(8):673-676. <https://doi.org/10.1130/G19704.1>
- Noffke N., Knoll A.H., Grotzinger J.P. 2002. Sedimentary controls on the formation and preservation of microbial mats in siliciclastic deposits: a case study from the Upper Neoproterozoic Nama Group, Namibia. *Palaio*, **17**(6):533-544. [https://doi.org/10.1669/0883-1351\(2002\)017%3C0533:SCOTFA%3E2.0.CO;2](https://doi.org/10.1669/0883-1351(2002)017%3C0533:SCOTFA%3E2.0.CO;2)
- Noffke N., Awramik S.M. 2013. Stromatolites and MISS – Differences between relatives. *GSA Today*, **23**:4-9. <https://doi.org/10.1130/GSATG187A.1>
- Noffke N., Beukes N., Gutzmer J., Hazen R. 2006. Spatial and temporal distribution of microbially induced sedimentary structures: a case study from siliciclastic storm deposits of the 2.9 Ga Witwatersrand Supergroup, South Africa. *Precambrian Research*, **146**(1-2):35-44. <https://doi.org/10.1016/j.precamres.2006.01.003>
- Noffke N., Chafetz H. 2011. Microbial mats in siliciclastic depositional systems through time. *SEPM Special Publication*, **101**:163-175. <https://doi.org/10.2110/sepm.sp.101>
- Olariu C., Steel R.J., Dalrymple R.W., Gingras M.K. 2012. Tidal dunes versus tidal bars: The sedimentological and architectural characteristics of compound dunes in a tidal seaway, the lower Baronia Sandstone (Lower Eocene), Ager Basin, Spain. *Sedimentary Geology*, **279**:134-155. <https://doi.org/10.1016/j.sedgeo.2012.07.018>
- Porada H., Bouougri E.F. 2007. Wrinkle structures: a critical review. *Earth-Science Reviews*, **81**(3-4):199-215. <https://doi.org/10.1016/j.earscirev.2006.12.001>
- Porada H., Ghergut J., Bouougri E.F. 2008. Kinneyia-type wrinkle structures—critical review and model of formation. *Palaio*, **23**(2):65-77. <https://doi.org/10.2110/palo.2006.p06-095r>
- Ribeiro A. 1997. *Estratigrafia e paleoambientes nas sucessões metassedimentares proterozoicas das serras do Lenheiro e São José, São João del Rei, Sul de Minas Gerais*. PhD Thesis, Universidade Federal do Rio de Janeiro, Rio de Janeiro, 167 p.
- Ribeiro A., Ávila C.A., Valença J.G., Paciuolo F.V.P., Trouw R.A.J. 2003. Geologia da Folha São João del Rei 1:100.000. In: Pedrosa-Soares A.C., Noce C.M., Trouw R., Heilbron M. (Eds.). *Projeto Sul de Minas, Etapa I: geologia e recursos minerais do sudeste mineiro*. Araxá: Companhia Mineradora de Minas Gerais, p. 521-622.
- Ribeiro A., Paciuolo F.V.P., Andreis R.R., Trouw R.A.J., Heilbron M. 1990. Evolução Policíclica Proterozóica no Sul do Cráton do São Francisco: análise da região de São João del Rei e Andreilândia, MG. In: Congresso Brasileiro de Geologia, **36**, Natal. *Anais*, p. 2605-2613.
- Ribeiro A., Teixeira W., Dussin I.A., Ávila C.A., Nascimento D. 2013. U-Pb LA-ICP-MS detrital zircon ages of the São João del Rei and Carandaí basins: new evidence of intermittent Proterozoic rifting in the São Francisco paleocontinent. *Gondwana Research*, **24**(2):713-726.

- Riding R. 2006. Microbial carbonate abundance compared with fluctuations in metazoan diversity over geological time. *Sedimentary Geology*, **185**(3-4):229-238. <https://doi.org/10.1016/j.sedgeo.2005.12.015>
- Sarkar S., Banerjee S., Chakraborty P.P. 2020. Microbial mat structures and role of microbes in Precambrian siliciclastic sedimentation. *Episodes*, **43**(1):164-174. <https://doi.org/10.18814/epiugs/2020/020010>
- Sarkar S., Banerjee S., Samanta P., Chakraborty N., Chakraborty P.P., Mukhopadhyay S., Singh A.K. 2014. Microbial mat records in siliciclastic rocks: examples from four Indian Proterozoic basins and their modern equivalents in Gulf of Cambay. *Journal of Asian Earth Sciences*, **91**:362-377. <https://doi.org/10.1016/j.jseaes.2014.03.002>
- Sarkar S., Samanta P., Altermann W. 2011. Setulfs, modern and ancient: Formative mechanism, preservation bias and paleoenvironmental implications. *Sedimentary Geology*, **238**(1-2):71-78. <https://doi.org/10.1016/j.sedgeo.2011.04.003>
- Scheidweiler D., Mendoza-Lera C., Mutz M., Risse-Buhl U. 2021. Overlooked implication of sediment transport low flow: Migrating ripples modulate streambed photo- and heterotrophic microbial activity. *Water Resources Research*, **57**(3):e2020WR027988. <https://doi.org/10.1029/2020WR027988>
- Seilacher A. 1999. Biomat-related lifestyles in the Precambrian. *Palaio*, **14**(1):86-93. <https://doi.org/10.2307/3515363>
- Smith B.J., Turkington A.V., Curran J.M. 2005. Urban stone decay: the great weathering experiment? *Geological Society of America – Special Paper*, **390**:1-9. <https://doi.org/10.1130/0-8137-2390-6.1>
- Soares A.C.P., Noce C.M., Trouw R.A.J., Heilbron M. 2002. *Carta Geológica São João Del Rei - Folha SF.23-X-C-II, Escala 1:100.000*. Projeto Sul de Minas - Etapa I. Araxá: Companhia Mineradora de Minas Gerais.
- Taj R.J., Aref M.A.M., Schreiber B.C. 2014. The influence of microbial mats on the formation of sand volcanoes and mounds in the Red Sea coastal plain, South Jeddah, Saudi Arabia. *Sedimentary Geology*, **311**:60-74. <https://doi.org/10.1016/j.sedgeo.2014.06.006>
- Tang D.J., Shi X.Y., Jiang Q., Wang X.Q. 2011. Morphological association of Microbially Induced Sedimentary Structures (MISS) as a paleoenvironmental indicator: an example from the Proterozoic succession of the Southern North China Platform. In: Noffke N., Chafetz H. (eds.). Microbial mats in siliciclastic depositional systems through time. *SEPM Special Publication*, **101**:163-175.
- Tarhan L.G. 2018. Phanerozoic shallow marine sole marks and substrate evolution. *Geology*, **46**(9):755-758. <https://doi.org/10.1130/G45055.1>
- Teixeira W., Sabaté P., Barbosa J., Noce C.M., Carneiro M.A., 2000. Archean and Paleoproterozoic evolution of the São Francisco Craton, Brazil. In: Cordani U.G., Milani E.J., Thomaz Filho A., Campos D.A. (eds.). *Tectonic Evolution of South America: International Geological Congress*, **31**:101-137.
- Thomas K., Herminghaus S., Porada H., Goehring L. 2013. Formation of *Kinneyia* via shear-induced instabilities in microbial mats. *Philosophical Transactions of the Royal Society A: Mathematical, Physical and Engineering Sciences*, **371**(2004):20120362. <https://doi.org/10.1098/rsta.2012.0362>
- Tolhurst T.J., Gust G., Paterson D.M. 2002. The influence of an extracellular polymeric substance (EPS) on cohesive sediment stability. In: Winterwerp J.C., Kranenburg C. (Eds.). *Fine sediment dynamics in the marine environment*. Amsterdam: Elsevier, p. 409-426.
- Tu C., Chen Z.Q., Retallack G.J., Huang Y., Fang Y. 2016. Proliferation of MISS-related microbial mats following the end-Permian mass extinction in terrestrial ecosystems: evidence from the Lower Triassic of the Yiyang area, Henan Province, North China. *Sedimentary Geology*, **333**:50-69. <https://doi.org/10.1016/j.sedgeo.2015.12.006>

ERRATUM

<https://doi.org/10.1590/2317-4889202220210034erratum>

In the manuscript “The impact of benthic microbial communities in sediment dispersion and bedform preservation: a view from the oldest microbially induced sedimentary structures in South America”, DOI: 10.1590/2317-4889202220210034, published in the Braz. J. Geol, 52(2):20210034:

Where it reads:

© 2021 The authors. This is an open access article distributed under the terms of the Creative Commons license.

It should read:

© 2022 The authors. This is an open access article distributed under the terms of the Creative Commons license.

Where it reads:

Braz. J. Geol. (2021), 52(2): e20200034

It should read:

Braz. J. Geol. (2022), 52(2): e20200034